



HAL
open science

Fractal cometary dust – a window into the early Solar System

Thurid Mannel, Mark S. Bentley, Roland Schmied, Harald Jeszenszky, Anny Chantal Levasseur-Regourd, Jens Romstedt, Klaus Torkar

► **To cite this version:**

Thurid Mannel, Mark S. Bentley, Roland Schmied, Harald Jeszenszky, Anny Chantal Levasseur-Regourd, et al.. Fractal cometary dust – a window into the early Solar System. *Monthly Notices of the Royal Astronomical Society*, 2016, 462 (Suppl. 1), pp.S304-S311. 10.1093/mnras/stw2898 . insu-01395718

HAL Id: insu-01395718

<https://insu.hal.science/insu-01395718>

Submitted on 18 Nov 2020

HAL is a multi-disciplinary open access archive for the deposit and dissemination of scientific research documents, whether they are published or not. The documents may come from teaching and research institutions in France or abroad, or from public or private research centers.

L'archive ouverte pluridisciplinaire **HAL**, est destinée au dépôt et à la diffusion de documents scientifiques de niveau recherche, publiés ou non, émanant des établissements d'enseignement et de recherche français ou étrangers, des laboratoires publics ou privés.

Fractal cometary dust – a window into the early Solar system

T. Mannel,^{1,2★} M. S. Bentley,^{1★} R. Schmied,¹ H. Jeszenszky,¹
A. C. Levasseur-Regourd,³ J. Romstedt⁴ and K. Torkar¹

¹Space Research Institute, Austrian Academy of Sciences, Schmiedlstrasse 6, 8042 Graz, Austria

²Physics Institute, University of Graz, Universitätsplatz 5, 8010 Graz, Austria

³UPMC (Sorbonne Univ.); CNRS/INSU; LATMOS-IPSL, BC 102, 4 place Jussieu, F-75005 Paris, France

⁴European Space Research and Technology Centre, Future Missions Office (SREF), Noordwijk, the Netherlands

Accepted 2016 November 7. Received 2016 November 5; in original form 2016 July 27

ABSTRACT

The properties of dust in the protoplanetary disc are key to understanding the formation of planets in our Solar system. Many models of dust growth predict the development of fractal structures which evolve into non-fractal, porous dust pebbles representing the main component for planetesimal accretion. In order to understand comets and their origins, the *Rosetta* orbiter followed comet 67P/Churyumov–Gerasimenko for over two years and carried a dedicated instrument suite for dust analysis. One of these instruments, the MIDAS (Micro-Imaging Dust Analysis System) atomic force microscope, recorded the 3D topography of micro- to nanometre-sized dust. All particles analysed to date have been found to be hierarchical agglomerates. Most show compact packing; however, one is extremely porous. This paper contains a structural description of a compact aggregate and the outstanding porous one. Both particles are tens of micrometres in size and show rather narrow subunit size distributions with noticeably similar mean values of $1.48^{+0.13}_{-0.59}$ μm for the porous particle and $1.36^{+0.15}_{-0.59}$ μm for the compact. The porous particle allows a fractal analysis, where a density–density correlation function yields a fractal dimension of $D_f = 1.70 \pm 0.1$. GIADA, another dust analysis instrument on board *Rosetta*, confirms the existence of a dust population with a similar fractal dimension. The fractal particles are interpreted as pristine agglomerates built in the protoplanetary disc and preserved in the comet. The similar subunits of both fractal and compact dust indicate a common origin which is, given the properties of the fractal, dominated by slow agglomeration of equally sized aggregates known as cluster–cluster agglomeration.

Key words: comets: general – comets: individual: 67P/Churyumov – Gerasimenko – planets and satellites: formation.

1 INTRODUCTION

Comets are among the most primitive bodies in our Solar system, likely to have preserved material from the growth processes in the protoplanetary disc. In particular, the investigation of the morphology of cometary dust particles is expected to provide insight into dust agglomeration in the early solar nebula.

Characterization of cometary dust has been performed by direct investigation of the particles collected by the *Stardust* mission (Brownlee et al. 2006) and a class of interplanetary dust particles (IDPs) collected in the Earth’s stratosphere supposed to be of cometary origin (Brownlee 1987; Bradley 2003), as well as by *in situ* exploration of their light scattering properties by the *Giotto* mission (Levasseur-Regourd et al. 1999; Fulle et al. 2000).

Characterization has also been indirectly obtained through analysis of remote light scattering observations (Dollfus 1989; Levasseur-Regourd et al. 1997, 2007; Kolokolova & Kimura 2010).

The resulting picture of cometary dust was that of a mixture of small compact particles and large agglomerates composed of submicrometre-sized subunits. The agglomerates are described by Flynn (2008) as generally weakly bound and by Brownlee (1987) and Hörz et al. (2006) as very porous. Reproduction of remote observations of solar light scattered by cometary dust by Lasue & Levasseur-Regourd (2006), Levasseur-Regourd et al. (2007) and Kolokolova & Kimura (2010) confirm these results and suggest a fractal construction. Fractal-like objects can be encountered in nature, e.g. as snowflakes, coastlines or the growth of cosmic dust particles (Mandelbrot 1982; Meakin 1983, 1991). Models and experiments predict that the onset of dust growth in the early Solar system is fractal (Dominik et al. 2007; Blum & Wurm 2008). However, the subsequent evolution of the dust particles is expected to compact and fragment the initial structures

* E-mail: thurid.mannel@oeaw.ac.at (TM); mark.bentley@oeaw.ac.at (MSB)

(Ormel, Spaans & Tielens 2007; Dominik 2009; Lorek et al. 2016). Experimental studies investigating the compaction of cosmic dust agglomerates predict that the resulting particles can maintain relatively high porosities but have lost their initial fractal structure (Blum et al. 2006).

For a direct detection, the fragile cometary dust particles had to survive the collection process. In the case of the *Stardust* mission, the particles suffered major alteration during collection (Brownlee et al. 2006), which destroyed all delicate, possibly fractal structures. However, the analysis of the tracks in the collection material suggests that about half of the detected cometary dust particles were highly porous aggregates (Hörz et al. 2006), which supports the possibility that comets stored fragile material. Similarly, although the collection process of IDPs is expected to preserve fragile material (Bradley 2003), most delicate structures might still be damaged.

The investigation of cometary dust particles collected in almost pristine state has now been addressed by the dust analysing instruments on board the comet orbiter *Rosetta*. Accompanying comet 67P/Churyumov–Gerasimenko between 2014 and 2016 through its perihelion passage, *Rosetta* studied dust particles at distances down to 10 km from the nucleus with relative velocities down to cm s^{-1} (Fulle et al. 2015). The three dedicated dust analysis instruments COSIMA (Cometary Secondary Ion Mass Analyzer; Hilchenbach et al. 2016), GIADA (Grain Impact Analyser and Dust Accumulator; Rotundi et al. 2015) and MIDAS (Micro-Imaging Dust Analysis System; Riedler et al. 2007; Bentley et al. 2016b) measured various properties of particles from nanometre to millimetre size, including their morphology, speed, momentum, optical cross-section and composition.

All three instruments found the dust particles to be agglomerates with different morphologies (Della Corte et al. 2015; Rotundi et al. 2015; Bentley et al. 2016b; Langevin et al. 2016). The aggregates with denser packing are called compact by GIADA and MIDAS (Della Corte et al. 2015; Rotundi et al. 2015; Bentley et al. 2016b), whereas COSIMA refers to particles which did not fragment and show well-defined shapes as compact (Langevin et al. 2016). COSIMA also detected irregular particles which fragment on impact and appear to comprise 10- μm -sized subunits (Hornung et al. 2016; Langevin et al. 2016). Their estimated tensile strength 1 kPa is rather low (Hornung et al. 2016), which underlines that cometary dust contains very fragile agglomerates. Overall, the morphology of cometary dust found by COSIMA and MIDAS shows great resemblance to IDPs (Bentley et al. 2016b; Langevin et al. 2016). Additionally, MIDAS and GIADA discovered and investigated a fractal cometary dust population. Whilst GIADA determined the physical properties such as size, speed and density of the fractals (Fulle et al. 2015, 2016a), MIDAS recorded the first direct image of a dust particle with an extremely open structure (Bentley et al. 2016b), which is now demonstrated to be fractal.

This work analyses the morphology of particles collected with MIDAS and establishes that at least one has a fractal structure. The findings are then interpreted with regard to common growth models for the early Solar system. The paper is organized as follows. Section 2.1 contains the data set consisting of 3D topographies of almost pristine cometary dust particles collected and imaged with MIDAS. Their fractal analysis is described in Section 2.2, and the results are summarized in Section 3. A comparison of the findings between the three dust analysis instruments of *Rosetta* and an interpretation regarding origin and evolution of the dust particles are given in Section 4. Finally, the conclusions can be found in Section 5.

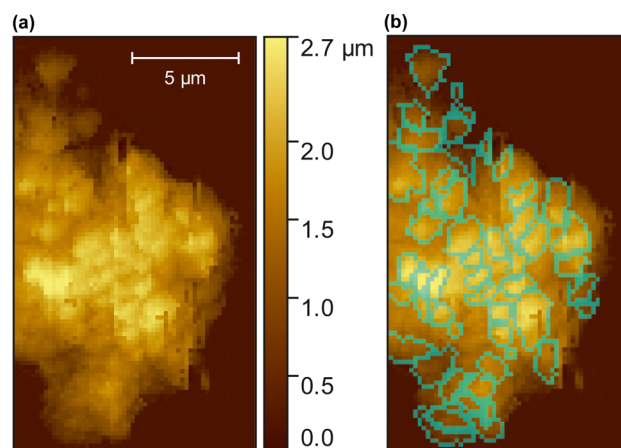


Figure 1. (a) Crop of a MIDAS post-processed topographic image showing particle F as example for the structure of compact agglomerates. The scan field measures $11.3 \times 19.6 \mu\text{m}^2$ and has a pixel resolution of 195 nm. The height is represented by the colour scale. The post-processing of the scan is described in Appendix B. (b) Corresponding area with the unequivocally detectable subunits outlined in light blue. The remaining body of the particle is assumed to be composed of similar subunits as the outlined ones, although there are areas where the existence of a matrix material cannot be excluded.

2 METHODS

2.1 Morphological analysis of dust from comet 67P

MIDAS, the atomic force microscope (AFM) on board *Rosetta* (Riedler et al. 2007; Bentley et al. 2016a), provided unique 3D topographies of nearly pristine cometary dust particles with sizes between tens of micrometres down to hundreds of nanometres (Bentley et al. 2016b). A first analysis of dust collected at comet 67P/Churyumov–Gerasimenko between 2014 September and the perihelion passage in 2015 August showed that cometary dust particles are hierarchical agglomerates of subunits with distinct sizes (Bentley et al. 2016b). However, the quality of the morphological data acquired by MIDAS allows a more detailed investigation of their structure, including fractal analysis.

In the pre-perihelion dust collection, roughly 10 particles were imaged which contain sufficient clearly identifiable subunits for analysis. Most of them show a dense packing and will hereafter be called compact agglomerates. An example of one such particle (hereafter particle F, where the naming follows the convention started in Bentley et al. 2016b) is presented in Fig. 1(a) and all visible subunits are marked in Fig. 1(b) (more information about the marking process can be found in Bentley et al. 2016b). A second particle, introduced in Bentley et al. (2016b) as particle E, shows an extremely open and flocculent construction. It is presented in Fig. 2(a) and a 2D projection of the subunits composing the particle is shown in Fig. 2(b). Unique amongst the entire pre-perihelion particle collection, particle E has a special structure which can be clearly identified as fractal.

2.2 Fractal dimension as description for dust growth

Although a fractal in the strict mathematical sense does not exist in nature, there are natural objects which can be described well by a fractal dimension (Mandelbrot 1982; Meakin 1983, 1991). Snowflakes are common examples for fractal structures in nature since they exhibit the same patterns at different locations, a

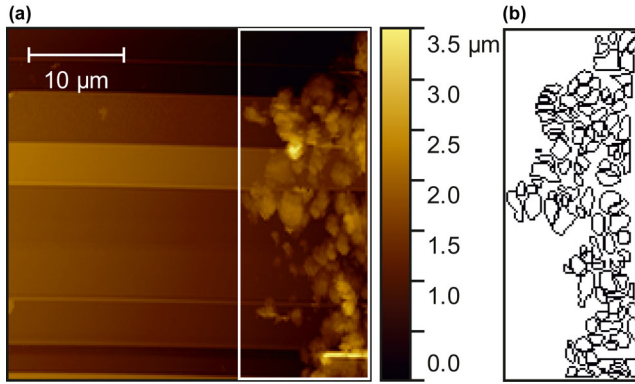


Figure 2. (a) Crop of a MIDAS post-processed (Bentley et al. 2016a,b) topographic image showing particle E. The scan field measures $38 \times 54 \mu\text{m}^2$ and has a pixel resolution of 210 nm. The height is represented by the colour scale. The horizontal stripes are scanning artefacts and do not alter the topography of particle E significantly. (b) Corresponding area to the white frame in (a), showing all identified subunits of particle E as 2D projection. Particles which are not visible in (b) are not found to be connected to particle E and thus are either individual dust particles or fragments (for further discussion, see Section 2).

behaviour called self-similarity. A special case of self-similarity, called scale invariance, describes the repetition of the same pattern when zooming into the structure. Most of the fractals in nature show self-similarity only in a statistical way and their scale invariance is limited to a small range of magnification factors. An example is a coastline (Mandelbrot 1967) whose pattern will never repeat exactly and not at any zoom; however, its structure is characteristic and follows a certain order. Similarly to the coastline, fractal dust agglomerates show a statistical fractal structure which extends over a few levels of magnification.

To calculate a fractal dimension Df for such a fractal dust agglomerate, it is generally accepted to use the particle mass m and size s relation

$$m \propto s^{Df} \quad (1)$$

if this relation is satisfied for different size scales (Meakin 1991; Blum 2006). The fractal dimension Df is always smaller than the Euclidean dimension of the particle which leads to structures which do not occupy the whole given space but are rather porous. Dust particles with a fractal dimension between 1 and 2 have chain-like structures beginning to fill a region but failing to occupy it completely, comparable to a knotted string or a ‘dust flake’. Equally, particles with fractal dimensions between 2 and 3 are not filled entirely but contain open voids which disappear as the fractal dimension tends to 3.

To calculate a fractal dimension which is comparable to values published from growth experiments or models, it is mandatory to use the same calculation method (Falconer 1990). Therefore, the fractal dimension of particle E will be determined by two common techniques: The correlation function, which is in the case of MIDAS data only slightly affected by uncertainties and described in Section 2.3, and the scaling relation, which is used to compare to the fractal dimension of the dust detected by GIADA (Fulle et al. 2016a) and described in Section 2.4. The determination of the fractal dimension of particle F is prevented by its compact structure; thus, an estimate of the dimension based on its topographic features will be given in Section 2.5.

The application of the correlation function and the scaling relation to MIDAS data leads to some challenges: MIDAS does not measure masses but topography, thus finding the relation between particle mass and size is only possible if a homogeneous density of all subunits is assumed. Also, MIDAS scans only the surface of a particle and not its internal structure, which prevents a survey of all subunits. This shortcoming is overcome by different techniques for the two methods of calculating the fractal dimension and is described in the respective sections. Finally, both herein analysed dust particles have only been imaged at one resolution, which prevents determination of the fractal dimension at different levels of magnification. Thus, scale invariance cannot be confirmed for these particles. However, as described in Section 4, the detection of particles with a similar fractal dimension but two orders of magnitude larger by GIADA (Fulle et al. 2016b) indicates that the structure of the fractal dust is scale invariant.

2.3 Calculation of the fractal dimension \widehat{Df} via the correlation function

A common way to calculate a fractal dimension of a dust agglomerate is the density–density correlation function (Meakin 1991; Aker 1996; Blum 2006). This approach is preferred for MIDAS data since it uses the relationship of the location of the subunits rather than their lateral extent. The latter suffers from a common uncertainty of AFM measurements called tip-sample convolution, an effect which can artificially broaden subunits with steep flanks (Bentley et al. 2016b). The correlation function also overcomes the issue that MIDAS only scans the surface and not the interior construction of the particle: the fractal dimensions of structures such as particle E, with a fractal dimension less than 2, can be derived from the 2D projection of the particle without introducing major uncertainties (see Appendix C for a discussion of this method and the induced uncertainties).

To apply the density–density correlation function

$$C(r) = \langle \langle \varphi(\mathbf{r}')\varphi(\mathbf{r}' + \mathbf{r}) \rangle \rangle_{r=|r|} \quad (2)$$

on MIDAS data, the function is interpreted as the probability to find two subunits with distance r in the particle, averaged over all positions \mathbf{r}' and all directions \mathbf{r} . MIDAS data are not continuous but sampled on a grid with a finite step size; thus, the probability of finding a subunit at point \mathbf{r} is simply $\varphi(\mathbf{r}) = 1$ if the grid point is occupied by a subunit, and $\varphi(\mathbf{r}) = 0$ if not.

As can be found in e.g. Meakin (1991) or Blum (2006), the correlation function scales for a homogeneous, self-similar fractal with

$$C(r) \propto r^{-(d-\widehat{Df})}, \quad (3)$$

where d is the Euclidean dimension of the space and is 2 for the presented calculation due to the use of a 2D projection. The fractal dimension \widehat{Df} is marked with a hat to indicate that it has been calculated with the correlation function rather than the scaling relation. For real dust particles with finite sizes the power-law behaviour will only extend over a certain length which depends on the overall size s and the size of the subunits s_0 of the structure (Meakin 1991; Aker 1996).

As shown in Aker (1996), the correlation function for data in a grid can be calculated from a normalized distribution of distances between the subunits. The number of subunits and the number of

Table 1. Size distribution of the subunits in particles E and F. Sizes are given as diameter of the disc with the equivalent area as the marked subunit. The smallest and largest size for the subunits of particle E are taken from Bentley et al. (2016b). For particle E, 112 subunits are considered, for particle F 52. The uncertainties contain the marking of the subunits in the scans and tip convolution, where the latter only broadens the features and thus leads to an asymmetric uncertainty interval. Details about the uncertainty calculation can be found in Bentley et al. (2016b).

Subunits of particle	Smallest size (μm)	Largest size (μm)	Mean (μm)
E	$0.58^{+0.15}_{-0.20}$	$2.57^{+0.04}_{-0.51}$	$1.48^{+0.13}_{-0.59}$
F	$0.66^{+0.29}_{-0.55}$	$2.29^{+0.08}_{-0.76}$	$1.36^{+0.15}_{-0.59}$

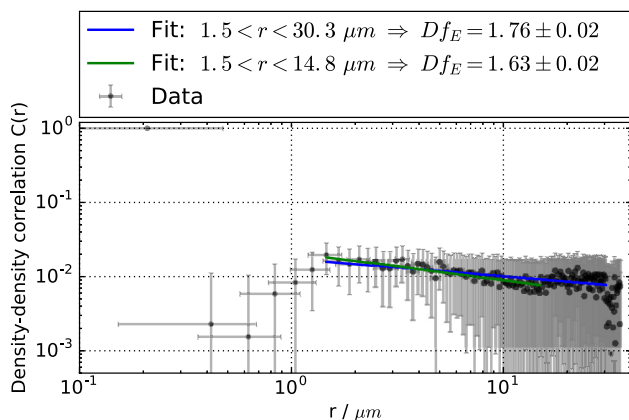


Figure 3. Density–density correlation function $C(r)$ of particle E. The expected power-law behaviour $C(r) \propto r^{d-\tilde{D}f}$ is only disturbed for largest distances r between subunits, which is expected due to the asymmetric shape of particle E. The derived fractal dimension depends on the fitted range of r , where the fits with the most extreme results are shown and constrain $\tilde{D}f_E = 1.7 \pm 0.1$. Error bars are taken into account by the fit and account for the unlikely cases where the distance of the subunits was strongly distorted either by tip convolution or a faulty identification of subunits on the scan.

grid points with distance r are described by $F(r)$ and $N(r)$, respectively. The correlation function becomes

$$C(r) = \frac{F(r)}{N(r)}, \quad (4)$$

which is again an averaged density over all distances and all directions (Aker 1996).

To calculate the fractal dimension of particle E via the correlation function, its subunits were identified as described in Bentley et al. (2016b). However, in contrast to Bentley et al. (2016b), no completely detached dust units were taken into account. This reduces the number of subunits to the 112 units depicted in Fig. 2(b). Whilst the latter publication contains a cumulative size distribution of all subunits, this paper presents the minimum, mean and maximum sizes of the herein evaluated 112 subunits shown in Table 1. The step size of 210 nm in the X- and Y-directions of the scan defines the grid for MIDAS measurement points, where the centre of each subunit defines one occupied grid point. The resulting correlation function is shown in Fig. 3 and follows the expected power-law behaviour for $1.5 \mu\text{m} < r < r_{\text{max}}$ for particle E. The lower limit is defined by the mean diameter of the subunits. The upper limit r_{max} should be determined by the overall size s of particle E; however, due to the asymmetric shape it is smaller. As visible in Fig. 3, r_{max} can be chosen up to

$30 \mu\text{m}$. Fitting the power-law behaviour for different r_{max} , a highest ($\tilde{D}f_E = 1.76 \pm 0.02$) and lowest ($\tilde{D}f_E = 1.63 \pm 0.02$) value for the fractal dimension can be found (see Fig. 3). This constrains the fractal dimension to $\tilde{D}f_E = 1.70 \pm 0.1$, where the uncertainties are calculated as given in Appendix D.

2.4 Calculation of the fractal dimension $\tilde{D}f$ via the scaling relation

A second approach uses the scaling relation (Blum 2006) and is carried out to allow a comparison with the fractal dimension calculated by GIADA (Fulle et al. 2016a). Following equation (1), this technique compares the mass of a particle to its fraction of filled space. Assuming that the particle is an agglomerate of equal subunits, the mass m is proportional to the number of subunits i . The size of the subunits is denoted as s_0 and the size of the whole particle is measured by s . A fractal particle then satisfies the scaling relation

$$i = k \left(\frac{s}{s_0} \right)^{\tilde{D}f}, \quad (5)$$

where k is a scaling parameter which depends on the way the particle size s is calculated and on the value of the fractal dimension. For cases similar to the presented one, k is commonly of the order of unity (Brasil, Farias & Carvalho 2000) and is thus set to 1 for the presented calculation. The tilde indicates that this fractal dimension has been derived via the scaling relation rather than the correlation function.

There are various ways in which a size s can be calculated, depending on the particle construction and other factors. In most calculations for dust aggregates, the radius of gyration s_g is used, where

$$s = s_g = \sqrt{\frac{1}{2N} \sum_{i=1}^N \sum_{j=1}^N |\mathbf{r}_i - \mathbf{r}_j|^2}. \quad (6)$$

In this equation, N is the number of subunits and \mathbf{r} is the positions of the subunits. The size of the subunits s_0 is measured by the radius of the disc with the same area as the subunit. Since the size distributions of the subunits of particles E is relatively narrow (see Table 1), s_0 can be taken as half of the mean subunit size.

As shown in Bentley et al. (2016b), the mean diameter of the subunits is slightly larger than their mean height; thus, in general, a stacking of subunits can be excluded. As visible in Fig. 2(a), it is even possible to see the target surface in between the single subunits. Thus, in the case of particle E, it is expected that the absolute majority of subunits can be probed due to the particle's porous monolayer character.

The radius of gyration of particle E is then $s_g = (10.73 \pm 0.06) \mu\text{m}$ and the mean subunit radius $s_0 = (0.74 \pm 0.30) \mu\text{m}$, which leads to a fractal dimension of $\tilde{D}f_E = 1.76 \pm 0.29$. The uncertainty is calculated as described in Appendix D.

2.5 Estimation of the fractal dimension for the compact particle

As MIDAS only probes topography, a rather compact structure such as that of particle F prevents the determination whether it has a fractal construction or not. The compact appearance of the particle does not exclude the structure being fractal since dust growth processes such as ballistic particle–cluster aggregation (BPCA) naturally produce fractal structures which seem as compact as particle F and exhibit fractal structures with dimensions close to 3 (Kozasa, Blum

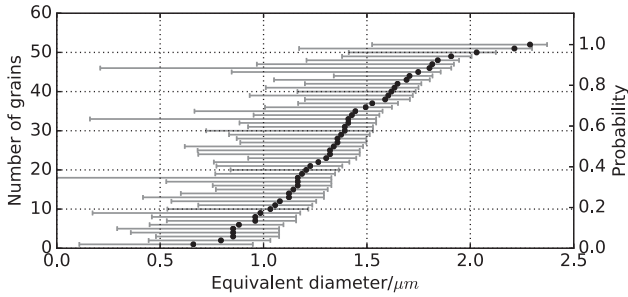


Figure 4. Size distribution of the subunits of particle F which are identified in Fig. 1. The left scale shows the cumulative number of subunits and the right scale the probability that a subunit has a size below the related value. The error bars depict the 1σ statistical and the systematic uncertainty; for details, see the Methods section of Bentley et al. (2016b).

& Mukai 1992). As particle F could well possess a fractal structure, or have possessed it prior to impact, a possible fractal dimension is estimated based on the topographic features of the compact agglomerate.

The projection of particle F shows no voids but rather a dense accumulation of many similar-sized subunits. The exact sizes of all identified subunits are shown in Fig. 4, where the smallest, largest and mean value can be found in Table 1. It is obvious that the tightly packed subunits fill a whole area without holes; thus, the fractal dimension of particle F can be assumed to be higher than 2.

Investigating the three-dimensional shape of particle F, its flatness is noticeable since its height of only of $3\ \mu\text{m}$ is much smaller than its lateral dimensions of 11 and $19\ \mu\text{m}$. As GIADA detects compact particles with oblate shapes exhibiting aspect ratios up to 10 (Fulle et al. 2016b), such a flat shape could indeed be pristine. However, a compact flat fractal agglomerate such as particle F would have a fractal dimension closer to 2 than to 3. If the flatness was not pristine but caused by compaction on impact, particle F must have had a higher porosity prior to collection. This would also imply a fractal dimension the closer to 2 the higher the initial porosity was.

Altogether, if particle F has a fractal structure, its fractal dimension prior to collection was probably between 2 and 3 with a tendency to the lower limit.

3 RESULTS

The fractal dimension of particle E is determined to be $\widehat{Df}_E = 1.7 \pm 0.1$ via a correlation function for the location of all subunits. Since a fractal dimension of less than 2 is a mathematical description of an agglomerate structure of loosely connected subunits possibly featuring holes, the topology of particle E is well represented.

Conversely, it is not possible to decide whether particle F has a fractal structure or not. Since not all subunits of the compact agglomerate are visible in the image, no fractal dimension was determined. However, if the particle has a fractal structure, a qualitative analysis of the topography suggests a fractal dimension between 2 and 3 with a favoured value closer to 2. Since particle F represents the structure of all compact agglomerates collected with MIDAS, this result underlines the low fractal dimension of particle E as prominent feature standing out the whole particle collection.

Despite the diversity in the constructions of particles E and F, the subunit sizes are similar and the size distributions rather narrow (see Table 1). Whilst the lower limit might be influenced by the resolution of the scans, the mean size and the upper limit show good agreement.

4 DISCUSSION

The cometary dust particle morphologies observed by MIDAS are in good agreement with the results of the other dust analysis instruments on board *Rosetta*. Particles showing a dense packing of subunits comparable to the compact agglomerate particle F have been detected at larger size scales (about $50\ \mu\text{m}$ to $1\ \text{mm}$, with subunit sizes larger than tens of micrometres) by COSIMA (Hilchenbach et al. 2016; Langevin et al. 2016) and GIADA (Della Corte et al. 2015; Rotundi et al. 2015; Fulle et al. 2016b). For the fractal particle E, a larger counterpart can be found in the GIADA data: a fraction of the detections is interpreted as generated by millimetre-sized, extremely porous ‘fluffy’ particles (Fulle et al. 2015). Their volume filling factor is determined to be as low as $\Phi \approx 10^{-4}$ and their equivalent bulk density $< 1\ \text{kg m}^{-3}$ (Fulle et al. 2015). Due to the nature of the GIADA data, the fractal dimension of the fluffy particles has to be inferred from modelled parameters using the scaling relation given in equation (5). The resulting value of $\widehat{Df}_{\text{GIADA}} \approx 1.8$ (Fulle et al. 2016a) is in excellent agreement with the fractal dimension found for the fractal particle E ($\widehat{Df}_E = 1.76 \pm 0.29$). The fact that a similar fractal dimension is observed for dust particles two orders of magnitude different in size strongly supports the existence of a fractal dust population since fractal dust growth should be scale invariant over a certain size range.

The direct detection of fractal cometary dust is an important finding for Solar system evolution and cometary growth models. Theory (Weidenschilling & Cuzzi 1993; Ormel et al. 2007; Dominik 2009) predicts that the initial dust growth in the early solar nebula always creates open and porous fractal structures and is supported by experimental work (Blum & Wurm 2008). The smallest building blocks are presumably of submicron size (Li & Greenberg 2003; Rietmeijer & Nuth 2004; Bentley et al. 2016b) and move uniformly with the flow of the gas in the protoplanetary disc. Their small relative velocities are induced by Brownian motion, which leads to hit-and-stick collisions. The developing dust agglomerates are predicted to have a fractal dimension close to 1.4 until they reach sizes of about $10\ \mu\text{m}$ (Blum et al. 1998; Krause & Blum 2004). From this size on their relative velocities grow due to radial drift, settling or turbulence in the protoplanetary disc. The emerging structures are characterized by a fractal dimension of approximately 1.7 (Blum et al. 1998), which is in excellent agreement with the value measured for the fractal particle E. However, it is expected that subsequent growth phases further process the dust. Fractal dust particles grow up to decimetres and gain relative velocities up to metres per second, which leads to compaction or fragmentation if they collide (Blum & Wurm 2008; Dominik 2009). The compaction phase has been experimentally investigated by Blum et al. (2006) who predict a rise of the volume filling factors to $\Phi = 0.20\text{--}0.33$, where agglomerates of non-spherical and polydisperse subunits tend to the lower limit. The compression evolves the fractal agglomerates to non-fractal, but still porous pebbles of roughly centimetre size (Ormel et al. 2007; Lorek et al. 2016). These pebbles are linked with the compact agglomerates found by GIADA (Fulle et al. 2016b). Their measured volume filling factor of $\Phi \approx 0.48$ (Fulle et al. 2016b) is higher than the predicted value, which might be the result of the incorporation of fragments created in collisions of the agglomerates (Dominik 2009). The smaller compact agglomerates detected by MIDAS such as particle F might stem from the same pebble population, which would suggest a non-fractal structure. The proposed common origin of the fractal and compact agglomerates is also supported by the similar size distribution and shape of the subunits of the fractal particle E and the compact agglomerate particle F (see

Table 1). Further growth from pebbles to kilometre-sized planetesimals or cometesimals needs to be initiated by a new process, the most promising of which is the gravitational instability (Johansen et al. 2007). An interesting feature of this scenario are the low velocities during comet accretion, which would naturally lead to the preservation of pristine structures.

Particle E is interpreted as a surviving pristine fractal dust particle which allows a view back to the early growth phases of our Solar system. Its fractal dimension $\widehat{D}f_E = 1.7 \pm 0.1$ and hierarchical construction of similar sized subunits (Bentley et al. 2016b) indicate a growth dominated by slow agglomeration of equally sized aggregates, known as cluster–cluster agglomeration (CCA; Blum 2006). The existence of fractal cometary dust indicates that not all dust particles are further processed to compacted pebbles. This could be a result of a slightly inefficient compaction process or a survival mechanism which has yet to be explained.

Particles E and F both show sizes of several tens of micrometres and have subunits of $1 \mu\text{m}$ which are expected to contain subunits of tenths of micrometre size (Bentley et al. 2016b) – a construction predicted for solar nebula condensates (Rietmeijer & Nuth 2004) but also for agglomerated interstellar dust (Clayton et al. 2003; Li & Greenberg 2003). Since a correlation between the occurrence of fractal dust particles and CO_2 has been suggested as possible data interpretation in Della Corte et al. (2015), the fractal particles may have been embedded in volatile ices during comet formation. This would imply that the fractal dust particles have been stored since their formation billions of years ago. They thus present a unique opportunity to study pristinely agglomerated, possibly interstellar dust.

5 CONCLUSIONS

The *Rosetta* mission offered the opportunity to investigate almost pristine cometary dust particles of comet 67P/Churyumov–Gerasimenko. The MIDAS AFM on board acquired the 3D topography of particles with sizes from tens of micrometres to hundreds of nanometres. A fractal analysis for particles collected between 2014 September and 2015 August which contain a sufficient number of subunits was presented in this paper.

One particle revealed an especially open and flocculent construction with a fractal dimension of 1.7 ± 0.1 . This result is in good agreement with the fractal dimension inferred for a whole population of particles surveyed by the GIADA instrument. A particle representative for tens of micrometre-sized compact agglomerates showed a structure which is either non-fractal or has a fractal dimension between 2 and 3. A more precise structural description for the compact agglomerates might be reached by analysis of dust collected later during the *Rosetta* mission.

The subunit size distribution of the fractal particle and the compact agglomerate particle are strikingly similar. They are rather narrow with an overall smallest subunit size of $0.58_{-0.20}^{+0.15} \mu\text{m}$ and largest size of $2.57_{-0.51}^{+0.04} \mu\text{m}$, where the mean subunit sizes are noticeably close with $1.48_{-0.59}^{+0.13} \mu\text{m}$ for particle E and $1.36_{-0.59}^{+0.15} \mu\text{m}$ for particle F.

The fractal particles are interpreted as preserved material from the early growth phases in the protoplanetary disc. Their hierarchical construction (Bentley et al. 2016b) and in this work determined low fractal dimension suggest growth dominated by slow CCA. A subsequent compaction and fragmentation phase evolves the majority of the fractal particles to compacted, non-fractal, centimetre-sized pebbles (Ormel et al. 2007; Blum & Wurm 2008; Dominik 2009;

Lorek et al. 2016) which represent the final stage of dust aggregation before a new process leads to integration into cometesimals and comets. The pebbles are linked with the compact agglomerates reported by GIADA (Fulle et al. 2016b) and possibly also the one to two orders of magnitude smaller compact agglomerates imaged by MIDAS.

The evolution of fractal particles to compact agglomerates implies a common origin for both populations, which is in good agreement with the similar subunit sizes determined by MIDAS. The subunits match the predicted sizes for interstellar dust agglomerates (Clayton et al. 2003; Li & Greenberg 2003) or solar nebula condensates (Rietmeijer & Nuth 2004). A suggested but not yet proven correlation of the release of fractals and supervolatile ices by Della Corte et al. (2015) would imply that the fractal particles are agglomerates of pristine interstellar dust.

ACKNOWLEDGEMENTS

We thank our referee who provided invaluable feedback and improved the readability of this article. We also appreciate the expertise of A. Rotundi and M. Fulle. *Rosetta* is an European Space Agency (ESA) mission with contributions from its member states and National Aeronautics and Space Administration (NASA). We also thank the Rosetta Science Ground Segment and Mission Operations Centre for their support in acquiring the presented data. Micro–Imaging Dust Analysis System (MIDAS) became possible through generous support from funding agencies including European Space Agency, PROgramme de Développement d’EXpériences scientifiques, the Austrian Space Agency, European Space Research and Technology Centre, the Austrian Academy of Sciences and the German funding agency Deutsche Agentur für Raumfahrtangelegenheiten. ACLR gratefully acknowledges support from the Centre National d’Études Spatiales (CNES, France) for this work, based on observations with MIDAS on board *Rosetta*. RS thanks the Austrian Research Promotion Agency (FFG) for financial support. TM and MSB acknowledge funding by the Austrian Science Fund FWF P 28100-N36, and TM acknowledges the Steiermärkische Sparkasse and the Karl-Franzens Universität Graz for their financial support. All data presented in this paper will be made available in the ESA Planetary Science Archive (<http://www.cosmos.esa.int/web/psa/psa-introduction> for manuals and <http://www.cosmos.esa.int/web/psa/rosetta> for the Rosetta database).

REFERENCES

- Aker E., 1996, PhD thesis, Univ. Oslo
- Bentley M. S. et al., 2016a, *Acta Astronautica*, 125, 11
- Bentley M. S. et al., 2016b, *Nature*, 537, 73
- Blum J., 2006, *Adv. Phys.*, 55, 881
- Blum J., Wurm G., 2000, *Icarus*, 143, 138
- Blum J., Wurm G., 2008, *ARA&A*, 46, 21
- Blum J., Wurm G., Poppe T., Heim L. O., 1998, in Ehrenfreund P., Krafft C., Kochan H., Pirronello V., eds, *Astrophysics and Space Science Library*, Vol. 236, Laboratory Astrophysics and Space Research. Kluwer, Dordrecht, p. 399
- Blum J., Schräpler R., Davidsson B. J. R., Trigo-Rodríguez J. M., 2006, *Adv. Phys.*, 652, 1768
- Bradley J. P., 2003, in Davis A. M., *Treatise on Geochemistry*, Volume 1. Elsevier, Amsterdam, p. 711
- Brasil A. M., Farias T. L., Carvalho M. G., 2000, *Aerosol Sci. Technol.*, 33, 440
- Brownlee D. E., 1987, *Phil. Trans. R. Soc. A*, 323, 305

- Brownlee D. et al., 2006, *Science*, 314, 1711
- Clayton G. C., Wolff M. J., Sofia U. J., Gordon K. D., Misselt K. A., 2003, *ApJ*, 588, 871
- Della Corte V. et al., 2015, *A&A*, 583, A13
- Dollfus A., 1989, *A&A*, 213, 469
- Dominik C., 2009, in Henning T., Grün E., Steinacker J., eds, *ASP Conf. Ser. Vol. 414, Cosmic Dust-Near and Far. Astron. Soc. Pac., San Francisco*, p. 494
- Dominik C., Blum J., Cuzzi J., Wurm G., 2007, in Reipurth V. B., Jewitt D., Keil K., eds, *Protostars and Planets V. Univ. Arizona Press, Tucson, AZ*, p. 783
- Falconer K., 1990, *Fractal Geometry—Mathematical Foundations and Applications*. Wiley, New York
- Flynn G. J., 2008, *Earth Moon Planets*, 102, 447
- Fulle M., Levasseur-Regourd A. C., McBride N., Hadamcik E., 2000, *AJ*, 119, 1968
- Fulle M. et al., 2015, *AJ*, 802, L12
- Fulle M., Altobelli N., Buratti B., Choukroun M., Fulchignoni M., Grün E., Taylor M. G. G. T., Weissman P., 2016a, *MNRAS*, 462, S2
- Fulle M. et al., 2016b, *MNRAS*, 462, 132
- Güttler C., Blum J., Zsom A., Ormel C. W., Dullemond C. P., 2010, *A&A*, 513, A56
- Hilchenbach M. et al., 2016, *ApJ*, 816, L32
- Hornung K. et al., 2016, *Planet. and Space Sci.*, 133, 63
- Hörz F. et al., 2006, *Science*, 314, 1716
- Johansen A., Oishi J. S., Mac Low M.-M., Klahr H., Henning T., Youdin A., 2007, *Nature*, 448, 1022
- Kolokolova L., Kimura H., 2010, *Earth Planets Space*, 62, 17
- Kozasa T., Blum J., Mukai T., 1992, *A&A*, 263, 423
- Krause M., Blum J., 2004, *Phys. Rev.*, 93, L021103
- Langevin Y. et al., 2016, *Icarus*, 271, 76
- Lasue J., Levasseur-Regourd A. C., 2006, *J. Quant. Spectrosc. Radiat. Transfer*, 100, 220
- Levasseur-Regourd A. C., Cabane M., Worms J. C., Haubebourg V., 1997, *Adv. Space Res.*, 20, 1585
- Levasseur-Regourd A. C., McBride N., Hadamcik E., Fulle M., 1999, *A&A*, 348, 636
- Levasseur-Regourd A. C., Mukai T., Lasue J., Okada Y., 2007, *Planet. Space Sci.*, 55, 1010
- Li A., Greenberg J. M., 2003, in Pirronello V., Krelowski J., Manicò G., eds, *Proc. the NATO ASI, Vol. 120, Solid State Astrochemistry*. Kluwer, Dordrecht, p. 37
- Lorek S., Gundlach B., Lacerda P., Blum J., 2016, *A&A*, 587, A128
- Maggi F., Winterwerp J. C., 2004, *Phys. Rev. E*, 69
- Mandelbrot B., 1967, *Science*, 156, 636
- Mandelbrot B. B., 1982, *The Fractal Geometry of Nature*. Freeman & Co., San Francisco
- Meakin P., 1983, *Phys. Rev.*, 51, L1119
- Meakin P., 1991, *Rev. Geophys.*, 29, 317
- Ormel C. W., Spaans M., Tielens A. G. G. M., 2007, *A&A*, 461, 215
- Poppe T., Blum J., Henning T., 2000, *ApJ*, 533, 454
- Riedler W. et al., 2007, *Space Sci. Rev.*, 128, 869
- Rietmeijer F. J. M., Nuth J. A., III, 2004, in Colangeli L., Mazzotta Epifani E., Palumbo P., eds, *Astrophysics and Space Science Library, Vol. 311, The New Rosetta Targets. Observations, Simulations and Instrument Performances*. Kluwer, Dordrecht, p. 97
- Rotundi A. et al., 2015, *Science*, 347, aaa3905
- Weidenschilling S. J., Cuzzi J. N., 1993, in Levy E. H., Lunine J. I., eds, *Protostars and Planets III. Univ. Arizona Press, Tucson, AZ*, p. 1031

APPENDIX A: PRISTINENESS OF PARTICLE E

As can be seen in Fig. 2, particle E was only partially scanned and is truncated at the right side. The scan shows no alteration of the particle; however, it was probably removed at the end of the scan

since the bottom is abruptly truncated and an attempt to rescan the area showed only few remaining fragments of the particle. Thus, all discussions and numbers refer only to the visible part of particle E in Fig. 2. Details about the scan and the post-processing can be found in Bentley et al. (2016b).

Particle E is extremely flat with maximal extents in the *X*-, *Y*- and *Z*-directions of $14 \times 37 \times 3 \mu\text{m}^3$ (Bentley et al. 2016b). This has two major implications. First, a possible alteration of the particle on impact cannot be excluded, and secondly, the calculation of the fractal dimension can be simplified by a 2D projection (see Section 2.3 and Appendix C).

The alteration of a dust particle colliding with another particle or with a dusty target has been investigated experimentally (Blum & Wurm 2000; Poppe, Blum & Henning 2000; Güttler et al. 2010); however, no studies are available for dust similar to particle E, namely a fractal consisting of irregularly shaped, submicrometre subunits. The general behaviour on collision is dependent on the relative velocity. For increasing collision velocities from millimetres per second to metres per second, first sticking occurs, then compaction and/or bouncing and finally fragmentation (Güttler et al. 2010). The incident velocity of particles collected by MIDAS is not known, and thus any possible alteration of a particle has to be inferred from the features in the scan and the GIADA velocity measurements for similar but larger dust.

If fragmentation occurred, either particle E is a fragment of a larger particle or particle E itself fragmented. If particle E was a fragment of a larger particle entering MIDAS, one would expect to detect more fragments on the target holding particle E. However, in a hundreds of micrometre distance to particle E, the target shows only four other particles which are all less than 5- μm -sized. Areas farther away from particle E have not been investigated. Thus, there are no other large particles detected which could indicate that particle E is a fragment of a larger particle. If particle E itself fragmented on collection, one would expect many subunit-sized particles close to the body of particle E.

The scan presented in Fig 2(a) shows only a few small detached dust units spread over the area. It is not clear if these are fragments or individual particles which have been collected in the same period. Thus, if fragmentation of particle E occurred, it was a minor alteration process resulting in the separation of a few subunits. Another possibility is that particle E represents the footprint created by a dust particle not detected by MIDAS. This scenario cannot be excluded and might happen, e.g. if a more compact particle bounces at impact on the target and leaves a porous upper layer or an attached fractal as footprint.

When inferring a possible collection speed of particle E through a comparison with GIADA data, it is important to note that the detected fluffy particles have sizes between 0.2 and 2.5 mm (Fulle et al. 2015), much larger than particle E. Nevertheless, their construction of many subunits assembled with a similar fractal dimension leads to the conclusion that the fluffy particles belong to the same population as particle E. The fluffy dust particles entered the GIADA instrument with velocities of a few centimetres per second (Fulle et al. 2015). Even if the collection velocity of particle E was higher, the sticking probability for an agglomerate of irregular, submicrometre small grains (such as particle E) is assumed to be larger (Blum & Wurm 2000; Poppe et al. 2000), allowing sticking at higher collision velocities. It seems likely that particle E had a rather low collection velocity, and thus did not undergo strong alteration on collection, which also suggests that the flat shape is at least partly pristine.

APPENDIX B: PRISTINENESS OF PARTICLE F

As visible in Fig. 1 particle F was only partially scanned. Since an attempt to re-scan it led to severe modifications of the particle, all calculations for particle F only refer to the scanned part shown in Fig. 1. The figure is a crop of a scan acquired on 2015 October 14 which was post-processed by a polynomial background subtraction to reduce surface tilt and curvature of the visible target area known to be flat. Additionally, after the analysis of the scan, an artefact was removed which did not influence the investigations but the quality of the visual presentation.

The size envelope of particle F is $11 \times 19 \times 3 \mu\text{m}^3$ and thus also flattened, which could be the result of compaction on impact. However, the associated low density compact agglomerates detected by GIADA show oblate shapes with aspect ratios up to 10 (Fulle et al. 2016b), indicating that the flat shape of particle F may not (purely) be a result of impact alteration. Unlike particle E, the target on which particle F was collected additionally contains a large number of similar particles of all sizes. Thus, the possibility remains that particle F is a fragment of a larger parent particle which compacted and fragmented on impact, creating many compacted fragments.

APPENDIX C: PROJECTION METHOD FOR PARTICLE E

Due to a funnel shielding, the MIDAS dust collection targets the deposition of all particles must have occurred with a velocity vector less than 15° from the target normal (hereafter defined as the z -direction). Since for particle E compaction but no major fragmentation is possible, it can be assumed that the subunits of the particle which extended in the z -direction might have rearranged on impact, which would mainly result in a compaction of the particle along this axis. Neglecting rearrangement in the X - and Y -directions as well as a possible onset of fragmentation, the compaction along the z -axis is treated like a projection of the particle along the z -direction.

Since for aggregates with fractal dimensions less than 2, it is possible to determine the fractal dimension from a 2D projection without introducing major uncertainties (Maggi & Winterwerp 2004), a compaction along the z -direction would not affect the calculation of the fractal dimension. The approach via a 2D projection can never yield a fractal dimension larger than 2 and has therefore to be treated with care. However, the structure of particle E is characteristic for a

fractal dimension less than 2, and thus the herein presented calculations of the fractal dimension are based on a 2D projection. Maggi & Winterwerp (2004) studied the behaviour of the fractal dimension of fractal particles with and without a two-dimensional projection and obtain an overestimation of the projected fractal dimension of typically 10 per cent. Since for particle E it is unknown how similar the initial and measured shape are, no estimation of the uncertainty of the projection is made. However, it should be kept in mind that the obtained value might be an overestimation by several per cent.

APPENDIX D: CONSIDERATION OF UNCERTAINTIES

The uncertainties of the fractal dimension of particle E via correlation function \widetilde{Df}_E are calculated by a propagation of the uncertainties affecting the location of the subunit centres. This includes the inaccuracy when identifying the single subunits on the scan and the uncertainty due to tip convolution which can broaden the size of MIDAS particles in rare cases up to 30 per cent (Bentley et al. 2016b). However, this broadening does not distort the determination of the centre of a subunit if it takes place uniformly in all directions. Estimating the heterogeneities of the shapes, tip convolution is calculated with 5 per cent of the value obtained in Bentley et al. (2016b). The measurement of the distance between the centres of the subunits on the scans is estimated to be accurate down to 1 pixel. The resulting uncertainty for the distance r between the subunits and the correlation function $C(r)$ is shown in Fig. 3 and taken into account by the orthogonal-distance regression fit. The final value $\widetilde{Df}_E = 1.70 \pm 0.1$ includes all mentioned uncertainties and the uncertainties introduced by the different results of the two most extreme fits.

The uncertainty of the fractal dimension of particle E via scaling relation \widetilde{Df}_E is propagated from the determination of the radius of the subunits to the radius of gyration and the fractal dimension. The uncertainty of the radius is generated by tip convolution which broadens the size up to 30 per cent as described in (Bentley et al. 2016b), and by marking two pixels in excess or missing two during the identification of the subunits on the scans. The resulting value $\widetilde{Df}_E = 1.76 \pm 0.29$ is dominated by tip convolution since the uncertainty caused by marking is an order of magnitude smaller.

This paper has been typeset from a $\text{\TeX}/\text{\LaTeX}$ file prepared by the author.